Pergamon

0969-806X(95)00424-6

Radiat. Phys. Chem. Vol. 48, No. 2, pp. 153–170, 1996

0969-806X/96 $15.00 + 0.00

ELECTRON PROCESSING OF FIBRE-REINFORCED ADVANCED COMPOSITES

AJIT SINGH,† CHRIS B. SAUNDERS, JOHN W. BARNARD, VINCE J. LOPATA, WALTER KREMERS, TOM E. McDOUGALL, MINDA CHUNG and MIYOKO TATEISHI

Research Chemistry Branch, AECL, Whiteshell Laboratories, Pinawa, MB, Canada R0E 1L0

Abstract—Advanced composites, such as carbon-fibre-reinforced epoxies, are used in the aircraft, aerospace, sporting goods, and transportation industries. Though thermal curing is the dominant industrial process for advanced composites, electron curing of similar composites containing acrylated epoxy matrices has been demonstrated by our work. The main attraction of electron processing technology over thermal technology is the advantages it offers which include ambient temperature curing, reduced curing times, reduced volatile emissions, better material handling, and reduced costs. Electron curing technology allows for the curing of many types of products, such as complex shaped, those containing different types of fibres, and up to 15 cm thick. Our work has been done principally with the AECL's 10 MeV, 1 kW electron accelerator; we have also done some comparative work with an AECL Gammacell 220. In this paper we briefly review our work on the various aspects of electron curing of advanced composites and their properties. Crown copyright © 1996 Elsevier Science Ltd.

INTRODUCTION

Radiation processing involves the use of natural and man-made sources of high-energy radiation on an industrial scale to give products that are safe, practical and beneficial (Silverman, 1981). In comparison to conventional processing methods, it is an energy conserving and environmentally benign technology. The number of electron accelerators in industrial use has been steadily increasing (Saunders, 1988; Leemhorst and Miller, 1990; Singh and Silverman, 1992), despite the fact that radiation-based technologies face close scrutiny by society and regulators. The growth of this technology has depended on normal market forces, which restrict the use of industrial electron and gamma processing to applications that either offer significant cost savings or produce unique and useful products. The major applications of this technology are based on: (i) polymerization or curing, e.g. coatings and rubber, (ii) crosslinking, e.g. wire and cable insulation, and plastic film, (iii) scission, e.g. degradation of Teflon and (iv) biological effects, e.g. sterilization of medical disposables (Silverman, 1981; Saunders, 1988; Stannett *et al.*, 1989; Cook, 1990; Schroeder, 1990; Tabata, 1990; Tenorth, 1990).

Radiation processing is a growing industry; in 1990, the value added to products by radiation processing was estimated to be in the billions of dollars (Cook, 1990). A large part of the credit for this growth belongs to the pioneers, who by their visionary work laid the foundation of industrial radiation processing of polymers, including Charlesby, Chapiro, Dole, Silverman, Stannett and Tabata [see Dole (1972, 1973), Kroh (1989), Singh and Silverman (1992), Woods and Pikaev (1994) for relevant references]. In the polymer industry, accelerated electrons are the main source of high-energy radiation (Saunders, 1988).

Advanced composites, such as carbon-fibre-reinforced epoxies, are being used for many applications, primarily because of their high strength-to-weight and stiffness-to-weight ratios, corrosion resistance, impact and damage tolerance characteristics, and wear properties (Margolis, 1986; Dostal, 1987). Applications for such thermosetting composites are found in the aircraft, aerospace, sporting goods, construction, transportation and automotive industries (Margolis, 1986). Though thermal curing of advanced composites is presently the dominant industrial process, electron curing of similar composites containing acrylated epoxy matrices has been demonstrated (Saunders *et al.*, 1988a, b; Saunders and Singh, 1989; Beziers and Capdepuy, 1990; Saunders *et al.*, 1991a, c, 1992; Singh and Saunders, 1992; Singh *et al.*, 1993). Radiation curing of advanced composites offers many advantages over thermal curing. Because of these advantages, radiation curing is emerging as an alternative to the currently popular thermal curing process. Though the focus of our work has been the aircraft industry, electron curing can also be used to make composites for the other uses mentioned above. Electron processing is compatible with the manufacture of composite products using traditional fabrication methods, including filament/tape winding, pultrusion and hand lay-up.

†Author to whom all correspondence should be addressed.

The basis of the radiation polymerization and crosslinking reactions is the formation of ionic and free radical intermediates in the polymeric substrates (Charlesby, 1960; Chapiro, 1962; Williams, 1968; Wilson, 1974; Woods and Pikaev, 1994)

Vinyl monomers $\rightsquigarrow$ Cations, Anions,

Free Radicals $\rightarrow$ Polymer (1)

Polymer $\rightsquigarrow$ Free radicals $\rightarrow$

Crosslinked polymer (2)

Of course, the main reaction path is accompanied by additional side reactions which produce scission, unsaturation, hydrogen, low molecular weight products, etc. (Dole, 1972, 1973; Wilson, 1974).

In this paper we review our work on radiation curing of carbon fibre-reinforced advanced composites. This work was started in late 1986 as a part of AECL's business development initiatives in the field of applications for 10 MeV electrons (Singh and Saunders, 1992). Our work was to support the development of markets for 10 MeV industrial electron accelerators (Kerluke and McKeown, 1993). Similar work has also been done by Aerospatiale in France, though their work was primarily focussed on filament-wound products and has remained largely proprietary (Beziers and Capdepuy, 1990).

Advantages of electron curing

Compared to thermal curing, many advantages have been identified for using electron curing (Saunders and Singh, 1989), as outlined below.

(1) *Curing at ambient temperature.* Tooling materials are required to control the dimensions and shape of a composite product. During the thermal curing cycle, the tool expands and contracts, often at a different rate, and to a different extent, than the composite product. During cooling, the matrix usually contracts to a different extent than the reinforcing fibre. These combined effects can change the dimensions of the product and create internal stresses, adversely affecting the composite properties (Weeton *et al.*, 1987). In principle, electron curing at ambient temperature can reduce these dimensional changes and the internal stresses in the produced composite. We have demonstrated reduced internal stresses in electron-cured composites (Saunders *et al.*, 1993b).

(2) *Reduced curing times.* A typical electron-curable carbon-fibre-reinforced acrylated epoxy laminate can be cured with a dose of about 100 kGy (Saunders *et al.*, 1993a). A commercially available 50 kW electron accelerator, whose typical availability exceeds 95%, can provide this dose to about 900 kg/h of material, assuming that 50% of the accelerator's electron beam energy is absorbed by the product being irradiated. By comparison, a typical autoclave can cure about 200 kg/h of material. Thus, the throughput for a 50 kW accelerator is much greater than that of a typical autoclave used for thermal curing. This is despite the products being cured one at a time during electron curing, compared to large batches in autoclaves.

(3) *Improved resin stability.* Most electron-curable matrix resins do not readily auto-cure at room temperature, making low-temperature storage unnecessary.

(4) *Reduction of volatiles produced.* Thermal curing of composites often produces volatile degradation products that can be hazardous and require appropriate controls (Weeton *et al.*, 1987). Electron curing drastically reduces the production of degradation products (Iverson *et al.*, 1992), though very small amounts of familiar industrial gases, such as hydrogen, carbon dioxide and methane, may be produced.

(5) *Better material handling.* Two factors that contribute to more efficient material handling during electron curing are: (i) the ability to handle the resins at room temperature makes it easier to fabricate composite products and (ii) the ability to electron cure each product as it is fabricated reduces the storage requirements for the uncured products. In the case of electron curing, products with different resins requiring different doses can be processed one after the other. In thermal curing, all the contents of the autoclave must have the same curing cycle.

(6) *Better material compatibility.* Products containing temperature-sensitive materials, e.g. foam or honeycomb containing low melting point polymers, or mixtures of fibres (such as mixed laminates with carbon fibre, polyethylene fibre, or aramid fibre reinforcement) can be easily electron cured without dimensional distortions. Thick laminates (up to 15 cm) have also been produced by electron curing (Saunders *et al.*, 1994). Thermal curing of such products, where possible, is challenging.

(7) *Reducing the processing costs.* Estimates suggest that the energy required for electron curing could be lower by a factor of five or more, with overall cost savings of the order of 30% (Saunders *et al.*, 1993b).

Challenges for electron processing

Electron processing of composites also faces some challenges, as listed below:

(1) *Availability of electron-curable matrix resins.* The epoxy formulations currently being used in the aircraft industry have been optimized for thermal curing and are not appropriate for electron curing. The thermal-curable epoxy formulations contain proton scavenging curing agents, such as

amines. Because they are typically kept refrigerated to prevent auto-cure, they also tend to absorb moisture during composite fabrication. Water, amines and other proton scavengers can interfere with the cationic polymerization of epoxies, during irradiation (Dickson and Singh, 1987). However, acrylated epoxy resins that are electron-curable via free radical mechanisms, are commercially available. The same range of properties for composites can be obtained using acrylated epoxy matrices, as with epoxy matrices (Beziers and Capdepuy, 1990; Saunders *et al.*, 1991a). Work is also being done to develop resins that undergo cationic curing on irradiation (Lapin, 1986; Crivello *et al.*, 1992; Walton and Crivello, 1994). However, the total number and variety of commercially available electron-curable resins remains much smaller than for the thermally cured resins.

(2) *Qualification procedures.* Extensive testing is required to develop electron-cured matrices for advanced composites that are truly equivalent to the conventional thermally cured matrices. The required criteria and qualification procedures for the aircraft industry are time consuming and expensive (Laramee, 1987; Traceski, 1987; Fila and Fews, 1993). However, this constraint may not apply to other uses of composites, e.g. in the transportation and automotive industries.

RADIATION PROCESSING

Whiteshell irradiator

The Whiteshell irradiator pilot scale facility, suitable for curing of small to quite large parts but at a low throughput, is shown in Fig. 1. This facility has been described previously (Barnard and Wilkin, 1987; Barnard and Stanley, 1989; Saunders *et al.*, 1991a). In our 10 MeV, 1 kW accelerator, a beam of electrons is accelerated horizontally, energy analyzed in a 270° bending magnet and projected downwards through a scanner which disperses the beam across the product as it passes by on a conveyor. The accelerator room is large enough to accommodate quite large parts for curing. However, most products are presented to the beam on a conveyor which accesses the accelerator room by way of a shielding maze.

The operations section of the facility is contained on a single basement level. Shielding of the workers in the accelerator control area is provided by poured in-place concrete. Shielding to the out-of-doors is provided mainly by an earth berm 3.5 m thick. A warehouse facility with loading bay is located at street level. The conveyor extends all the way from the warehouse onto the basement level, through the maze to the accelerator and back out through the maze and back to the warehouse. Dosimetry and quality assurance laboratories, and offices are also provided on the basement level. An AECL Gammacell 220 provides gamma irradiations for comparative dose rate studies.

Radiation protection

In general, the radiation protection objectives are the same for all types of accelerators used in radiation curing, namely, to provide protection to the worker and public from direct exposure to the beam or intense X-rays which might cause immediate harm, and to keep radiation doses as low as reasonably achievable (the ALARA principle). These objectives are achieved by providing sufficient shielding to maintain dose rates at negligible levels during operation, insuring that a set of administrative procedures for operating the facility safely are in place, and installing a set of fail-safe redundant interlocks to prevent personnel from inadvertent exposure to high radiation levels (IAEA, 1982, 1992).

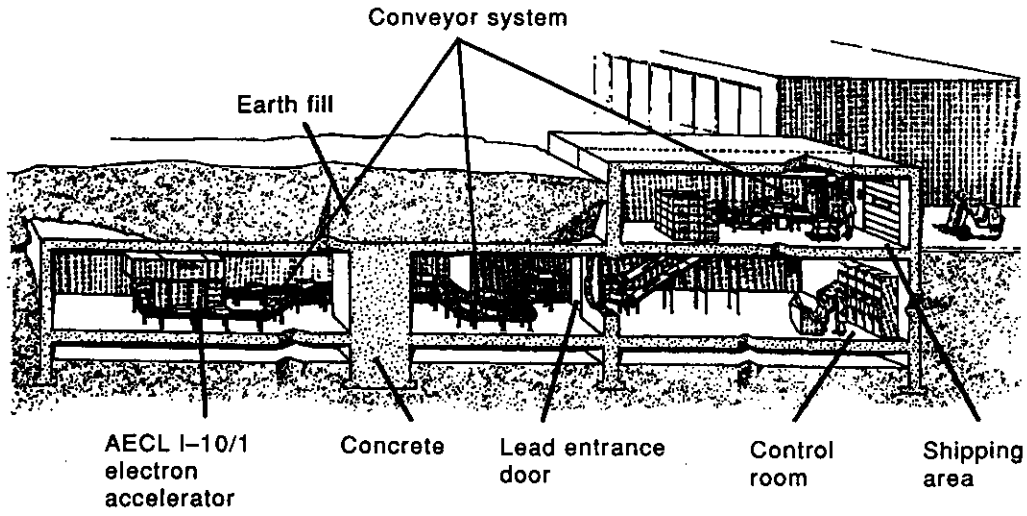

Fig. 1. Diagram of the I-10/1 accelerator facility.

Beyond these objectives are radiation protection considerations which are dependent on the type of radiation curing to be carried out and the type of equipment required. If thin composites are to be produced, low energy electrons are sufficient to penetrate the part. For thicker parts, higher energies will be required to penetrate the part or X-rays may be needed to achieve a uniform cure. As the energy is increased to improve penetration, the amount of shielding required to protect against X-rays and the likelihood of producing radioactivity either in the product being cured or the equipment also increases (Swanson, 1979).

The electron beam

Even for low power electron accelerators exposure of personnel to the direct electron beam is harmful. The strict adherence to procedures and a functioning interlock system are the primary protection against this hazard. However, for high power accelerators, the amount of heat generated by the impact of the beam is sufficient to melt metal components, explosively spall concrete and do other structural damage to the facility. Therefore, water-cooled beam dumps are required to protect building components. For 10 MeV beams with power greater than 20 kW, the intensity of X-rays produced from completely stopped electron beams in a beam stop may be sufficient, depending on the geometry of the beam strike area, to cause overheating of the shielding. Beam stops must be made thick enough to stop the electrons as well as partially attenuate the X-ray intensity. In such situations, damage could result from loss of coolant flow. The accelerator should therefore be interlocked to cease operation on low coolant flow in the beam stop.

X-rays

The term X-ray used here describes both the consequences of ejection of a bound electron by a high energy electron and "bremsstrahlung", the photons emitted by deceleration of the fast electrons by the nucleus of the target atoms/molecules (Swanson, 1979). For all practical purposes, as far as designing the shielding is concerned, it is the "bremsstrahlung" that needs to be protected against. The intensity of X-rays and, hence, the thickness required for adequate shielding increases with beam intensity and the atomic number of the target material. For a 10 MeV electron beam, for example, a lead target is about 3 times more effective in producing X-rays than an aluminum target (Swanson, 1979).

Energy also determines how effectively X-rays can penetrate materials and the thickness of the shielding required to provide protection. When electrons impinge on a target, the X-ray spectrum produced is continuous from a few tens of keV (the minimum energy of X-rays that can escape a thick target) up to a cutoff corresponding to the maximum energy of the electron beam. The average X-ray energy from a 5 MeV electron accelerator is about 1 MeV; these X-rays have about the same penetration ability as ^{60}Co gamma-rays. The average X-ray energy from a 10 MeV beam is about 4 MeV. The X-ray absorption coefficient (a measure of loss of energy to the absorber) decreases up to about 10 MeV and then increases as the probability of pair production increases with energy. However, the increased effectiveness of shielding of higher energy X-rays is offset by the onset of "showers" or "cascades", whereby increased X-ray intensity is produced from electron–positron pairs created in the target or the shielding (NCRP, 1977; Swanson, 1979).

Direct penetration of shielding is not the only consideration in designing shielding for worker protection. X-rays can scatter along mazes provided for product transport to the beam. Mazes must be long enough and provide enough scatters for X-rays to afford comparable attenuation to the shielding provided for the direct penetration path. Service ports for cabling and ventilation ducts must also be tortuous in order to prevent beams of X-rays from being scattered from the irradiation zone into the working areas.

A number of materials are available for shielding against X-rays. The shielding material of choice is concrete because it is easy to form and pour to shape, is relatively cheap, is widely available, and presents reasonable attenuation for the amount of shielding weight required. Lead is a good choice for local shielding where the most reduction for the amount of volume available is required. However, lead is very heavy, has a low threshold for photo-disintegration and, when shielding higher energy beams, contributes to neutron and proton production by way of the (γ, n) and (γ, p) reactions (NBS, 1973). While contributing to neutron production, lead itself is a relatively poor material for shielding neutrons (NCRP 1977; Swanson, 1979).

In some cases it is possible to save costs on shielding materials by taking advantage of the existing terrain (by recessing into the side of a hill, for example) and use earth berms as shielding. On a per unit weight basis, compacted or undisturbed earth is about as effective as concrete. However, if the lay of the land can not be exploited and earth has to be hauled to provide the shielding, it usually proves more costly than concrete.

A variety of other materials, including water, can be used as shielding materials (NCRP, 1977). Typically, steel or lead with steel stiffening is used for shielding doors. Shielding curves for many materials are available from several sources (NCRP, 1977; Swanson, 1979; Nucleon Lectern, 1984). These references also give rules of thumb and computational methods for estimating scattering or streaming along mazes and conduits. For low atomic number materials, it is generally acceptable to derive shielding curves from a material by scaling according to its density, from the shielding data of a material of

similar atomic number. However, care must be taken for converting shielding curves where the materials differ widely in atomic number, because it is the electron density that determines the effectiveness of a material for shielding against X-rays (Swanson, 1979).

Neutrons

X-rays from electron beams produce both neutrons and protons by photo-disintegration (γ, n and γ, p reactions). Since protons are heavy charged particles, their linear energy transfer to the medium is high and they lose energy very rapidly as they traverse materials. Most do not escape the target materials in which they are formed. Neutrons, however, are neutral particles and are much more penetrating. Since they can be produced by accelerated electron beams, attention to shielding for neutrons is also required (Swanson, 1979).

Except for some notable cases, the threshold energy for most photo-disintegration reactions in low atomic number materials lies above 10 MeV. These exceptions are deuterium (threshold energy: 2.23 MeV), beryllium (threshold energy: 1.67 MeV) and ^{13}C (threshold energy: 4.9 MeV) (NBS, 1973). Beryllium, a very toxic metal, is seldom encountered under normal electron-curing circumstances and the abundances of deuterium and ^{13}C are very low in nature. However, if electron-curing is conducted at energies higher than 10 MeV to enhance penetration, care must be taken in considering what extra shielding may be needed to protect against the neutrons that may be produced. As energies are increased above 10 MeV, more and more common elements of low atomic weight will photo-disintegrate, increasing neutron production and induced radioactivity. None of the above mentioned reactions should present a problem in electron-curing of plastics and composites up to 10 MeV in energy.

In general, the best neutron shielding materials are high in hydrogen because they effectively absorb neutron energy in elastic scattering reactions. Again, concrete is excellent because of its high water content (NCRP, 1977). Paraffin wax, oils, and organic solids also make good neutron shielding material. Their disadvantages are that they are generally flammable.

A general rule of thumb in shielding facilities using electron beams up to 20 MeV is that if the shielding is sufficient for the X-rays produced, it will also be sufficient for the neutrons produced. However, if a shielding maze is provided for product transport in and out of the irradiation room, then the shielding may not be sufficient because most shielding materials backscatter neutrons more efficiently than X-rays (Swanson, 1979). In such cases an analysis of scattering of both X-rays and neutrons along the maze (NCRP, 1977) must be carried out to show that the protection against scattered radiation afforded by the maze is comparable to the protection the bulk shielding provides against directly penetrating radiation, and that together, the two components of leakage radiation satisfy the design criteria for work place radiation fields established to meet the national standards for worker radiation protection.

Radioactivity

The production of neutrons usually accompanies the production of induced radioactivity. Many of the reaction products of photo-disintegration are radioactive. Also, the neutrons are absorbed by materials in the shielding and targets to create activation products by way of the n, γ reaction.

At low atomic weights most of these radioactive species are short-lived and decay away with half-lives ranging from seconds to days. However, in the time between production and decay, activation and photo-disintegration products in targets, beam lines and production materials can be the source of significant radiation fields. There is also the potential for inhalation or ingestion of radioactivity if materials that have been activated by the beam are machined or ground before the radioactivity has been allowed to decay. Swanson (1979) provides complete tables for estimating saturation activities as a function of energy and beam power for electron beam incident on a variety of target materials including concrete, steel, air, water and various elements. These tables also provide half-lives and the threshold energies for the production of each radioactive product.

The air of the facility can also be activated. The threshold for $^{14}N(\gamma, n)^{13}N$ reaction is 10.55 MeV. The half-life for the decay of ^{13}N is 9 min. In general, this should not present a hazard for workers since the highest concentrations are produced in the beam strike area where the X-radiation is most intense, and under normal circumstances will be vented away immediately following shutdown of the accelerator. However, it could contribute significantly to the worker's dose as an external source of radioactivity in which the worker is immersed for very brief periods following accelerator shutdown, provided the time gap between the accelerator shut down and the worker entry is short. The time for safe re-entry following shutdown of the electron beam depends on the rate of air exchange, the beam energy, the beam power and the duration of the beam as well as the half life of ^{13}N. Swanson (1979) provides tables for estimating maximum permissible concentration in accelerator room air, from ^{13}N as well as some higher energy photo-disintegration and activation products, based on the recommendations of the International Commission on Radiological Protection in ICRP Publication 2 (ICRP, 1960).

Although induced radioactivity in products exposed to 10 MeV electrons, or X-rays produced from them, would be negligible, it may be useful to check the product handling equipment in the target area, periodically, for any induced radioactivity build-up.

Radiation protection programs

Radiation protection programs at an electron accelerator facility should be drawn up in advance, to monitor and protect the worker from the anticipated radiation hazards. This means that limits on processing energy and the maximum beam power should be established in the planning stages. The degree of hazard based on the consequences of credible accidents should be estimated in advance. Mitigating measures and safety procedures should be implemented prior to first processing. A period of commissioning should also be provided with operational tests planned in advance and carried out, to demonstrate the safe operation of the facility as predicted in the safety analysis.

A good radiation protection program will contain the following elements (IAEA, 1982; IAEA, 1992): (i) workplace monitoring for radiation fields and radioactivity, (ii) worker dose monitoring, (iii) regular review and assessment of the sources of worker dose with corrective action to maintain doses as low as reasonably achievable, (iv) training in operational safety and safety equipment use, (v) a quality program which controls the risk at a very low or negligible level, and (vi) accident and near-miss investigation to prevent injury or its recurrence.

Industrial safety

A number of industrial safety hazards associated with electron curing are readily evident. These include toxic gases, machinery, fire, electrical equipment, pressurized systems, and flooding. Provision must be made to protect the worker from these hazards as well as from ionizing radiation. The following sections discuss three of the most commonly encountered hazards. Any or all of them may be present in an electron accelerator facility.

Machinery

One of the principal advantages of electron-curing is process speed. This makes the use of product handling equipment a necessity. Equipment such as high speed winders and conveyors offer the opportunity for entanglement of worker clothing and hair or the capturing and pinching of extremities. All process equipment should be designed to current national safety standards. The design of unique custom-made equipment for the facility should be analyzed separately as part of the safety analysis to identify in advance, and mitigate wherever possible, potential for injury in its use.

Toxic gases

There are two principal sources of toxic gases and vapours in an electron processing facility: volatiles from the product and toxic gases generated by ionizing radiation in air.

Heat generated by the beam and from the exothermic curing reactions induced during irradiation tends to elevate the temperature of the product and drive off the solvents and the uncombined monomers remaining after the cure is completed. These are released into the air of the irradiation room as airborne pollutants. Most of these pollutants may be toxic to some degree, the liver being the principal organ at risk, and may have adverse effects on the health of workers. Threshold limit values for chemical substances and physical agents in work place air are recommended by the American Conference of Governmental and Industrial Hygienists (ACGIH, 1993), and its counterparts in most countries.

Ventilation is the best protection against these toxic gases. For materials irradiated under vacuum, the evolution of volatiles directly from the part being processed is restricted by the vacuum envelope. However, it is good industrial hygiene practice, in this case, to discharge vacuum pumps directly to the exhaust ventilation duct of the target room. Normally the levels are not high enough to warrant environmental abatement in the form of charcoal or resin absorbers. However, for large scale production, workplace and effluent monitoring of off-gases and vapours from the product should be undertaken, at least initially, to determine if further action is warranted.

The two principal toxic gas species produced by ionizing radiation in air are nitrogen oxides and ozone (Brynjolfsson *et al.*, 1971; Swanson, 1979). The G values for nitrogen oxide and ozone are 4.8 and 10.3 molecules/100 eV respectively. The threshold limit values (TLV) for nitrogen oxide and ozone are 3 and 0.1 μg/g respectively. Because ozone is more toxic by an order of magnitude, and produced in greater quantities, it is the one that is generally targeted for control of workplace exposure (Swanson, 1979).

Ventilation is the best protection against the toxic gases produced. The facility ventilation should be balanced so that the net flow of supply air is always into the irradiation room and the total facility exhaust is out of the irradiation room. For very high power electron accelerators, the concentrations of ozone in air outside the facility may also represent a hazard to personnel or the environment. This may be mitigated by dilution with fresh air from outside because ozone decomposes back to molecular oxygen with a half-life of about 1 h, or ozone can be reduced back to O_2 before discharge by the use of recombiners. Guidance is given by Swanson (1979) for calculating the production and airborne concentrations of O_3 in electron accelerator facilities.

Fire

The injection of large quantities of energy from the electron beam into products consisting of flammable resins and combustible reinforcing materials presents the potential for setting of fire. If the product being cured is large, the fire can rapidly become intense, fuelled by the resins under cure and supplied with

oxygen from the ventilation air. The presence of highly oxidizing ozone will tend to accelerate combustion. The heat can become intense with the fire confined in a relatively small area in the irradiation room, or may be driven along the ductwork by the ventilation air to break out elsewhere in the facility. Normally, the combustion of the part in process will result in heavy smoke and airborne toxic vapour in the target room which can quickly overcome personnel attempting to respond to the fire. Self contained breathing apparatus should be provided, easily accessible near the facility entrance. Personnel should be trained in its use.

Therefore, fire detection systems should be designed to monitor for both smoke and temperature rise rate. Fire detection is further complicated in the high radiation environments of the accelerator room because some fire detection instrumentation, particularly smoke detectors, are subject to deterioration in radiation fields. It may be necessary to replace some components on a regular basis or ensure in some other way (by shielding, perhaps) that the protection they afford is always available. From this point of view, continued surveillance of the target room, particularly the target area, with a TV camera (which is common at many accelerator sites) assumes an important safety role.

The accelerator operation and the curing process should always be monitored by an operator on duty to insure that the product movement is not interrupted. The beam cannot be permitted to rest in one area long enough to induce burning. Normally the product handling system is interlocked to trip the accelerator if the product stops moving in the beam, or power to the product handling system is lost during production.

PREPARATION OF COMPOSITES

Materials

The carbon fibre types used in our work are; AS4, IM6, and IM7, in the following weaves: unidirectional, plain, and 5-harness satin, all from Hercules Inc. The resins used in our work are: CN104 and C-3000 (epoxy diacrylate oligomer), CN114 (epoxy acrylate), CN964 (acrylated urethane), S-297 (1,3-butylene glycol dimethacrylate), S-399 (dipentaerythritol monohydroxy pentaacrylate), S-604 (polypropylene glycol monomethacrylate), C-2000 (C_{14}-C_{15} diol diacrylate), C-5000 (polybutadiene diacrylate) and C-9503 (aliphatic urethane diacrylate) from Sartomer Inc; FW3 (blend of epoxy acrylates, methacrylates and acrylates), and BMI1 and BMI4 (blends of epoxy acrylates and bismaleimides) from Applied Poleramic Inc.; and electron-curable adhesives from Loctite Corporation and Union Carbide. A proprietary acrylated isocyanate coupling agent was prepared by us.

Laminate fabrication

We fabricate laminates using two methods, prepreg and resin transfer moulding (RTM).

Prepreg preparation. We have used two of the commonly used methods, wet-layup and solvent prepregging, for the fabrication of the laminates (Dostal, 1987).

Wet-layup method. In this method the fabric, with the desired resin poured on the fabric, is laid between two sheets of Vac-Pak HS-8171 bagging film (Richmond Aircraft Products). If the resin is not excessively viscous, it is manually spread throughout the fabric. When the resin is too viscous, the resin/fabric is placed on a heating pad and the resin viscosity is adjusted by controlling the temperature of the pad. Once the viscosity of the resin has been sufficiently reduced, the resin is spread manually throughout the fabric.

Solvent method. In this method, the fabric is placed in a polyethylene tray of the same size as the desired laminate panel. For routine laboratory scale work, we usually place 7 layers of fabric in one tray. The resin to be used is dissolved in an appropriate solvent. In the case of acrylated epoxies, acetone is a good solvent to use; for the BMI resins, chloroform works well. The resulting solution is then poured over the fabric in the tray and the solvent is then allowed to evaporate. In both cases the tray is placed in a heated oven at 70°C. This is to ensure that all the solvent is driven off, and that there is no moisture incorporated in the laminate during the solvent evaporation process.

Bagging prepreg. Once made, the prepreg with the fibre in the desired orientation is placed on aluminum plates which have been treated with a release agent. Most common mould release agents can be used for this purpose, up to a dose of 200 kGy. A sealant tape (e.g. Tacky Tape 5126-2, Schnee-Morehead Inc.) is placed around the edge of the aluminum plate. Once the prepreg has been laid to the desired thickness, a release fabric such as B-4444 (Richmond Aircraft Products) or perforated release film such as A5000 (Richmond Aircraft Products) is placed over the prepreg. A breather cloth such as RC-3000-20 (Richmond Aircraft Products) is placed over the release film or cloth. A vacuum port is then incorporated in the setup. This consists of a Swagelok 1/4 inch quick-disconnect coupler. A vacuum bag film (e.g. Vac-Pak HS-8171, Richmond Aircraft Products) is then placed over the laminate lay up. A vacuum system is then connected to the vacuum port and the bag evacuated. The laminate is evacuated for approximately one hour to provide some consolidation of the fabrics as well as to remove any air between the fabric layers. This also helps remove any traces of the solvent and moisture remaining in the prepregs. The laminate is then rolled with a rolling pin to provide further consolidation. Once this procedure is complete, the laminate is irradiated under vacuum using the electron accelerator.

Resin transfer moulding. In order for RTM to be used, a resin with a viscosity of 1 Pa s or less is required. In some cases, where the resin viscosity is too high, the resin is heated to decrease its viscosity. The fabric to be used is cut to the specified dimensions and placed in the tool to the thickness and fibre orientation required. The tool is then closed, the various hoses for resin transfer and vacuum are attached, and the tool is evacuated, which removes air, solvents, and any traces of water. Once the pressure is down to approximately 1 kPa, the resin is introduced either under its own flow or under pressure. Care is taken to ensure that no air enters the system. The resin is allowed to flow continuously into the tool until the resin exits on the vacuum side without air bubbles. At this point, the resin pressure is reduced. The resin and vacuum lines are then sealed. The tool is taken to the accelerator and the panel cured.

Atmosphere. Acrylated epoxies cure via free radical mechanisms (Dickson and Singh, 1987). Thus, as expected, oxygen inhibits the gel formation in an acrylated epoxy formulation on gamma irradiation (Saunders *et al.*, 1991b). However, the inhibition is negligible on electron irradiation (Saunders *et al.*, 1991b). For all practical purposes, our work on electron curing of composites has been done under inert atmosphere. Either the samples are vacuum-bagged, or the samples are under mechanical pressure between metal plates which prevents diffusion of oxygen into the bulk of the sample.

RESIN AND COMPOSITE TESTING

Several testing methods have been used to evaluate the resins and composites, as described below.

Sample preparation. Resin samples for gel fraction and size exclusion chromatography (SEC) were placed in sealed, evacuated pyrex test tubes. Samples for dynamic mechanical analysis (DMA) were prepared by pouring the resin into aluminum moulds and curing them under inert atmosphere. All samples were irradiated using either the Gammacell (dose rate: 7.8 kGy/h) or the I-10/1 electron accelerator (dose rate: 5.4 MGy/h) as described earlier (Singh and Saunders, 1992; Saunders *et al.*, 1993a). The preparation of carbon fibre prepregs has been described above. Thick composite samples (>70 ply) have also been prepared using the CN104 acrylated epoxy resin, to study possible variations in both absorbed dose and properties through the thickness of the cured laminates (Saunders *et al.*, 1994), in a similar manner. The samples for electron curing and X-ray curing were consolidated using standard vacuum bagging techniques, and external pressure was applied as needed. Samples were irradiated to doses from 0.1 to 1000 kGy, as required.

Gel fraction/size exclusion chromatography. Cured polymer samples (1 g) were crushed and placed in a pyrex glass tube containing tetrahydrofuran (THF). In the case of the composites, 2 g samples were cut and placed in pyrex glass tubes containing THF. The sample was heated overnight at 65°C, and the liquid extract was collected for SEC. A fresh aliquot of THF was added to the sample for another 24 h extraction at 65°C to remove any residual soluble fraction. After the second extraction in THF, the liquid was drained off, the resin sample was dried overnight under vacuum at 100°C, cooled and weighed, to determine the gel fraction. For SEC of the THF extract, the mobile phase used was THF at a flow rate of 1 ml/min. A 10 μl sample was injected using a Waters WISP 710B Injection System. Separation of the different molecular weights was done using Phenogel 5 500A (500–10,000 Dalton) and Phenogel 5 100A (50–1000 Dalton) Phenomenex 300 × 78 mm columns. Two different detectors were used in this work; a laser light scattering detector (Dawn F, Wyatt Technologies) and an index of refraction detector (Hewlett Packard 1047A). The signals from both the detectors were sent to a personal computer. Wyatt Technologies ASTRA software was used for the data acquisition and EASI software was used for the data analysis. The response of the SEC columns was calibrated using polystyrene molecular weight standards (800–233,000 Dalton) and biphenyl (154 Dalton). Soluble (Sol) fractions were calculated from the areas under the SEC curves for each dose. Figure 2 shows a typical SEC chromatogram obtained using the laser light scattering detector and the index of refraction detector.

Mechanical testing. Mechanical testing of electron-cured polymers and composites is done according to the ASTM testing methods (ASTM, 1984; tensile properties, D638M; flexural properties, D790M; compressive properties, D695). These tests were carried out at an aircraft manufacturer's testing laboratory.

Dynamic mechanical analysis. This method gives information about the rheological properties of ma-

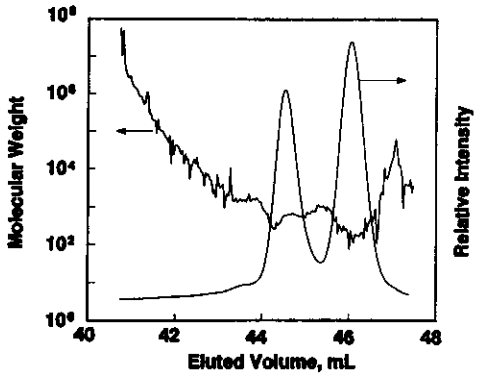

Fig. 2. Typical SEC chromatogram of polymer extractables. The molecular weight curve is obtained from the laser light scattering detector; the relative intensity curve is obtained from the index of refraction detector. The refractive index curve suggests that there are two major products and at least one minor product.

terials. We have used this method extensively, particularly for the composites and resins. The normal mode is to measure the flexural modulus as the temperature is increased or cycled (Fig. 3; Rheometrics, 1990; Mayer *et al.*, 1990). The standard tool used is the dual cantilever with zero stress and strain. The results obtained from the scan give flexural modulus, glass transition temperatures (tan δ, loss modulus), and service temperature for the material being studied. The service temperature is defined as the temperature at which the flexural modulus is 50% of the room temperature value.

Void content. Qualitative analysis of the void content is carried out by using the C-scan method (Henneke, 1987). This non-destructive method shows areas of porosity in the composites. By comparing the overall attenuation of the signal from the component being tested with the signal from a known sample with zero voids, relative overall porosity of the component can be determined. For more accurate determination of porosity our laboratory uses mercury intrusion porosimetry to determine the void content of composites. The instrument used is an Autopore II 9220 (Micrometrics), which can measure 4 samples at a time in 4 h. It gives the pore size distribution and the total void content for the composite being tested. Figure 4 shows a typical output showing the void size distribution for a composite sample. The instrument is capable of measuring pore sizes between 360 and 0.003 micrometers in diameter.

Curing dose determination

We have determined the curing dose for resins and composites by three methods: (1) gamma calorimetry, (2) DMA, and (3) Barcol Hardness (ASTM D2583; ASTM, 1984). The first two methods can be used for both resins and composites, while the third method is used only for composites.

Gamma calorimetry. We have developed an empirical method to quickly screen the curing dose of a large number of resin formulations. If the resin polymerizes on irradiation in the Gammacell, the resulting temperature rise curve provides the induction dose (gel point), the dose at 50% cure, and an indication of the polymerization process (single or multi-step curing process, slow or fast polymerization). From this information, one can calculate the electron beam curing dose for the neat resin and the fibre-reinforced composite, using an empirical formula derived during the development of this method (see later).

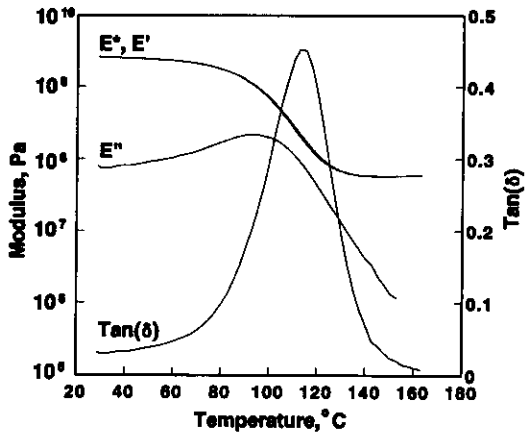

Fig. 3. Dynamic mechanical analysis curves for CN104 epoxy diacrylate resin: E^*—flexural modulus; E'—storage modulus; E''—loss modulus; tan δ-E''/E'.

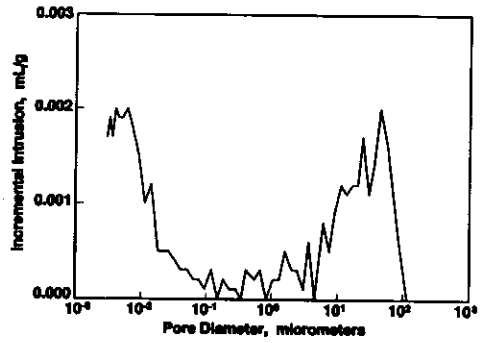

Fig. 4. Void size distribution for FW3 acrylated epoxy RTM composite using unsized, plain weave, 3 K, AS4 fibre, obtained by mercury intrusion porosimetry.

For the calorimetry measurements (Fig. 5), the resin to be investigated is placed in a Pasteur pipet which has been sealed at one end. The pipet is placed in an insulated jacket which can hold up to 9 samples. Beside each resin sample a K-type (chromel-alumel) thermocouple is placed, approximately 1 cm from the bottom of the sample tube. In every run, one of the samples is a reference which consists of a cured resin in an identical vial, to monitor normal temperature fluctuations in the Gammacell. The thermocouples are wired into a multichannel datalogger which is connected to a computer. The computer stores the voltages from the thermocouples as a function of time. Once the samples are setup, they are placed in the Gammacell 220 chamber and lowered into the radiation field. As the resin polymerizes, heat is evolved, causing an increase in temperature, and the voltage which is related to the temperature. When the exothermic polymerization reactions seem to have been completed, the samples are taken out of the Gammacell. Analysis of the thermal data is carried out using a spreadsheet program.

The signal from the reference resin is subtracted from that of the sample being investigated and is then converted to temperature. Figure 6 shows the temperature rise curve for S-297 (1,3-butylene glycol dimethacrylate), obtained by this method. From the curve, two values are used to determine the electron beam curing dose. One value is the gel point, the dose at which the temperature begins to rise. The second value is the dose at which the maximum temperature rise occurs. By applying equation (3), which we have

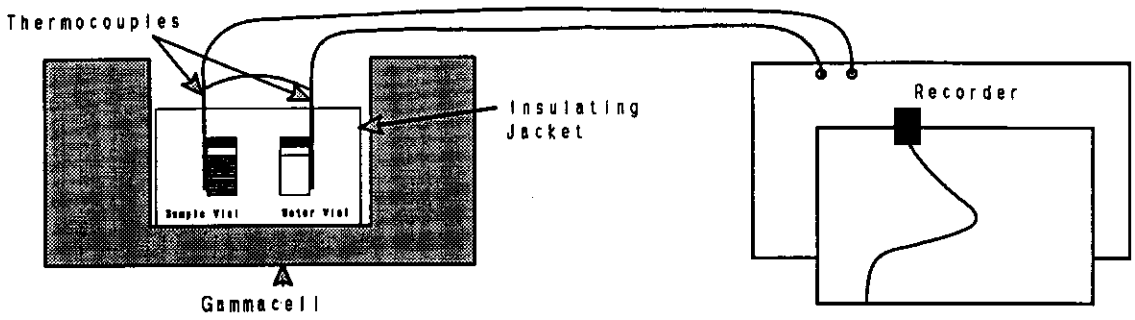

Fig. 5. Experimental setup for gamma calorimetry.

derived empirically, one can determine the approximate dose required to cure the resin. Generally, the composite curing dose is about 30 kGy more than that for the neat resin, for unsized fibre. For sized fibre, the curing dose is even higher (another 30 kGy or more, depending on the resin).

$$D_{100} = DGP + 10(10^{(DTM - DGP)}) \quad (3)$$

where D_{100} = dose at 100% cure, DTM = dose at maximum temperature rise (50% cure), DGP = dose at gel point.

Table 1 shows a comparison between the estimated curing dose from gamma calorimetry and the actual electron curing dose determined by DMA. With a slight modification to the sample chamber, this method can also be used to study the radiation curing of composites.

Dynamic mechanical analysis. For the determination of the curing dose, the flexural modulus and the glass transition temperatures derived from the DMA curves are important (Fig. 3). The temperatures at the peaks are the glass transition temperatures, $T_g(E'')$ and $T_g(\delta)$. This data allows us to plot the T_g values vs dose. The dose at which the glass transition temperature plateaus is considered the curing dose for the system being studied (Rheometrics, 1990). This method can be used to determine the curing dose for both resins and composites. The method is viewed as one of the more accurate ways of determining the curing dose of a system. However, this method is time consuming because each specimen must be analyzed separately. Depending on the T_g of the specimen, each analysis can take up to 3 h to complete. Figure 7 shows a typical plot of glass transition temperatures vs dose.

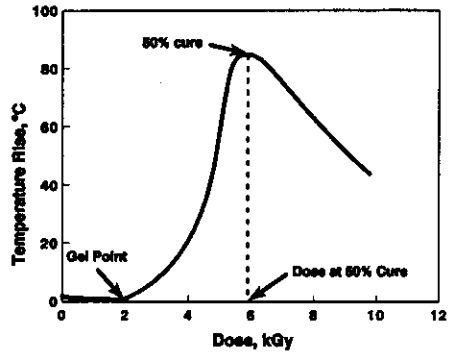

Fig. 6. Gamma calorimetry: temperature variation for S-297 (1,3-butylene glycol dimethacrylate), as a function of dose.

Barcol hardness. This method (ASTM, 1984; D2583) is a qualitative test to determine if a composite has been adequately cured. In this method, the Barcol Impressor is used to make measurements over a large area of the composite. Typically, one makes 10–100 hardness measurements over an area of 100–1000 cm^2, though it is easy to make an even larger number of measurements, over the desired area of the composite. Normally, if the hardness reading is 65 or greater, the dose received by the composite indicates that the part has been fully cured. Figure 8 shows a comparison of Barcol hardness with T_g values for FW3 acrylated epoxy composite as a function of dose. For more accurate determination, the hardness for each resin system employed at full cure needs to be determined.

Resin shrinkage

As monomers and oligomers polymerize, shrinkage occurs with the formation of chemical bonds. The normal Van der Waals spacing between molecules is approximately 3.4 Å. With polymerization, the spacing is reduced to approximately 1.34 Å, the distance between the C—C atoms (Sadhir and Luck, 1992). The degree of shrinkage (density increase) depends on the monomer size. The larger the original monomer, the smaller the overall shrinkage.

Shrinkage of the resin is one of the main contributors to internal stresses in composites. In thermally-cured systems, it has been concluded that up to 70% of a resin's shrinkage will occur below the gel point (Luck and Sadhir, 1992). Below the gel point, the resin still has mobility to allow the resin to shrink without incurring any internal stresses. Above the gel point, the resin becomes increasingly immobile and the stresses from shrinkage are then locked in the structure.

We have determined how the radiation-cured resin systems behave as compared to the thermal-cured resins. Figures 9–11 show the effect of dose on the

Table 1. Comparison of estimated with actual curing dose

Resin	Gel point (kGy)	Dose at temp. max. (kGy)	Estimated curing dose (kGy)	Actual curing dose (kGy)	Maximum temperature rise (°C)
S297	1.3	4.1	29	20	29.5
C3000	0.3	3.7	90	100	35.0
S604	0.5	3.1	26	30	44.7
FW3	1.1	4.2	40	45	27.3
BMI4	0.4	1.9	56	50	6.5

temperature rise and density changes for three resins; S-297 (1,3-butylene glycol dimethacrylate), S-604 (polypropylene glycol monomethacrylate) and BMI4 (acrylated bismaleimide). The data show that increases in the density and temperature due to polymerization occur at similar doses. From other studies, the gel point (dose at which crosslinking starts) results show that the onset of the temperature rise and crosslinking occur at the same dose. This indicates that, as expected, the density starts to increase as crosslinking begins. The maximum polymerization and crosslinking as denoted by the highest density values occurs at a much higher dose than the dose for the maximum temperature rise. It has been determined, using gel fraction measurements, that the maximum temperature rise occurs at ~50% gel fraction point (Figs 12 and 13). Further irradiation was required to achieve full polymerization/crosslinking of the resin. Comparing the density and temperature curves, we conclude that no significant shrinkage occurred below the gel point.

For the density measurements on the resins S-297, 604 and BMI4, 20 ml of monomer was placed in glass vials and capped. The samples were irradiated in the Gammacell at various doses. The dose rate was 110 Gy/min. The densities of the liquid resin and composite samples were determined by the ASTM D-792 procedures (ASTM, 1984).

Temperature rise during composite cure

As expected, there is also a rise in the temperature of the fibre-reinforced acrylated epoxy composite samples during radiation curing (Saunders *et al.*, 1991, 1994). The actual temperature rise depends on the resin being used, the resin loading, and the thickness of the composite. However, the temperature rise can be reduced if the required electron dose is given in several fractions, allowing the sample to cool between the irradiations (Saunders *et al.*, 1991b). In more recent work on thick samples (up to 15 cm thick; Saunders *et al.*, 1994), the temperature rise was found to be up to 132°C for a 2.5 cm thick sample when cured with a single electron dose of 50 kGy; however, the temperature rise was much lower (40°C) on X-ray curing (which takes a much longer time due to its lower dose rate and thus allows the heat generated to dissipate).

Our work has shown that multiple passes do not affect the properties of the material. Figure 14 shows the DMA curves for the same acrylated resin, cured to the same dose in a single pass and in multiple passes. Figure 14(a) shows the curves where the curing dose has been delivered in a single pass of 70 kGy. Figure 14(b) shows the same resin with the dose delivered in 7 passes of 10 kGy each. In this case the flexural moduli and glass transition temperatures are identical for both methods of delivering the dose.

Dose rate effect

Dose rate affects the kinetics of free radical polymerization reactions (Chapiro, 1962; Williams, 1968). From a practical point of view, the higher the dose rate, the lower the time of irradiation. Therefore, it is important to determine whether the curing characteristics of the various resins that can be used as the matrix materials for fabricating composites are dependent on the dose rate. We have examined the dose

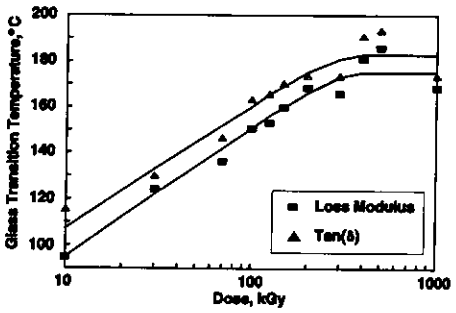

Fig. 7. Effect of dose on the glass transition temperature for the composite laminate with FW3 acrylated epoxy matrix.

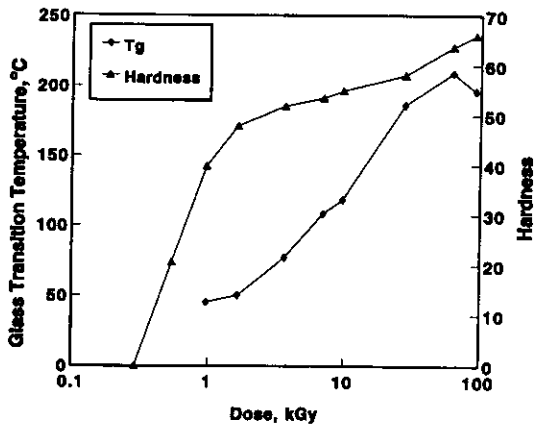

Fig. 8. Comparison of glass transition temperatures and barcol hardness for the composite with FW3 acrylated epoxy matrix.

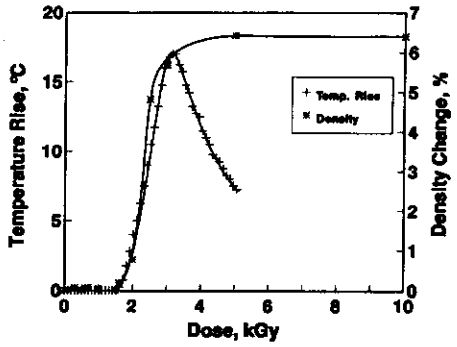

Fig. 9. Gamma calorimetry: effect of dose on the temperature rise and density change of S-604 (polypropylene glycol monomethacrylate) resin.

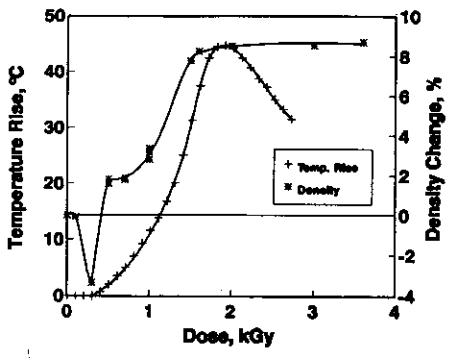

Fig. 11. Gamma calorimetry: effect of dose on the temperature rise and density change of BMI4 (acrylated bismaleimide) resin.

rate effect on the curing characteristics of some of the resins used in our work. In the case of the epoxy diacrylate based formulations, it was found that to reach a similar gel fraction, a much higher dose was needed on gamma irradiation, than on electron irradiation (e.g. 8 vs 60 kGy, for 90% gel fraction in C3000; Saunders *et al.*, 1991c). However, in the case of S-297 and S-604, the dose required for gamma irradiation is lower, as shown by the data in Figs 15–19. In the case of BMI1, the gel fraction of the neat resin is not affected by the dose rate; however, the gel fraction formation in the composite is more efficient on electron curing (Fig. 20). As mentioned earlier, at lower dose rates, the temperature rise in the irradiated samples is lower (Saunders *et al.*, 1994).

Crosslink density

The crosslink density (v) and the average molecular weight between crosslinks (M_c) can be estimated from the equilibrium elastic modulus (G'_e) of the cured resin. This modulus is assumed to be the minimum value of the flexural modulus for the polymer, above its T_g. According to the kinetic theory of rubber elasticity (Ferry, 1970)

$$G'_e = g_n RTv = g_n RT\rho/M_c \qquad (4)$$

where G'_e = equilibrium elastic modulus (dynes/cm^2), g_n = a numerical factor (1.0083), R = gas constant [8.31×10^7 dynes/(cm K mol)], T = absolute temperature (K), v = crosslink density (mol/cm^3), ρ = resin density (g/cm^3), M_c = molecular weight between crosslinks (g/mol). The crosslink densities and the molecular weights between the crosslinks can also be determined for the composites of these resins (Pater *et al.*, 1991) by using the following formula:

$$T_g = T_{go} + k_1 v = T_{go} + k_2 M_c^{-1} \qquad (5)$$

where T_g = glass transition temperature, T_{go} = a constant, k_1 = crosslink density constant, k_2 = molecular weight constant, v = the crosslink density in crosslinks per cm^3, M_c = the molecular weight between crosslinks.

From the plots of the T_g, using tan(δ), vs crosslink density or molecular weight between crosslinks, the crosslink constants for the resin can be derived and those for FW3 are given in Table 2.

Radiation effects on FW3 resin and its composites

The data on the effect of electron treatment on the gel fraction, the T_g and the molecular weight distribution of the extractables from FW3 resin, cured to doses ranging from 0.1 to 1000 kGy is shown in Fig.

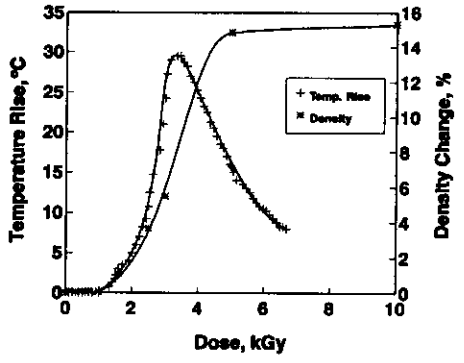

Fig. 10. Gamma calorimetry: effect of dose on the temperature rise and density change of S-297 (1,3-butylene glycol dimethacrylate) resin.

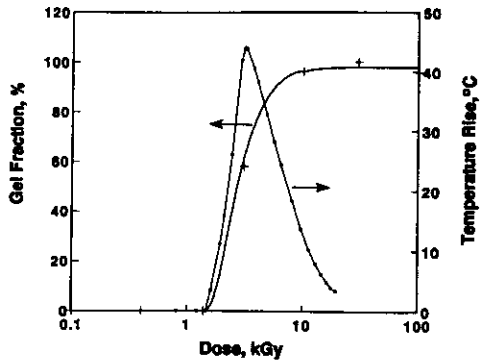

Fig. 12. Comparison of temperature rise with gel fraction of the gamma irradiated S-604

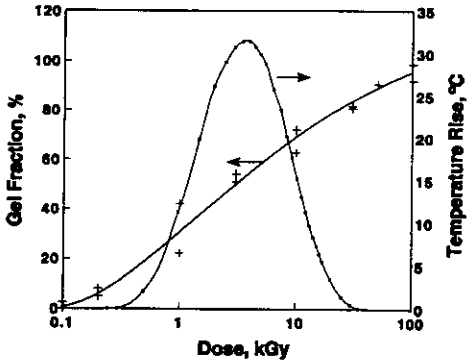

Fig. 13. Comparison of temperature rise with gel fraction of the gamma irradiated C-3000 resin.

21. The maximum T_g for the FW3 polymer, based on the tan δ curve, is about 190°C, occurring at a dose of about 150 kGy. The gel fraction curve shows that the maximum gel content, greater than 99%, is also reached at a dose of about 150 kGy. The SEC data shows that the molecular weight distribution of the extractables is continually changing, up to a dose of about 100 kGy. The molecular weight curves are automatically expanded by the data acquisition software to 100% height; their total amount is equal to the Sol level (100-gel fraction %), at the noted dose. The molecular weight of the extractables is constant above 100 kGy.

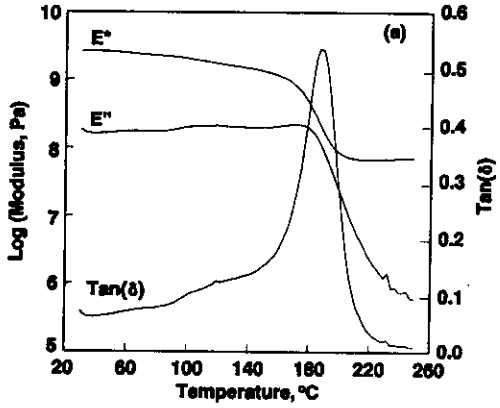

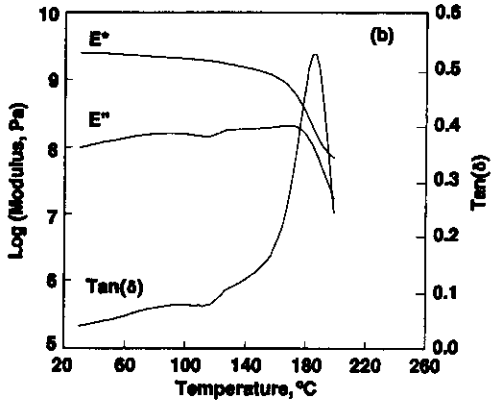

Fig. 14. Comparison of delivering the curing dose in a single or multi-pass protocol, to a proprietary acrylated epoxy resin: (a) 70 kGy in a single pass. (b) 70 kGy in seven passes (10 kGy each)

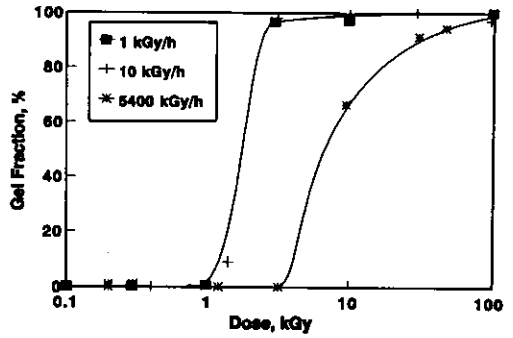

Fig. 15. Dose rate effect on the gel fraction of the S-297 (1,3-butylene glycol dimethacrylate) resin.

Figure 22 shows the effect of electron treatment on the gel fraction, the T_g and the molecular weight distribution of the extractables from the AS4 fibre-reinforced composite samples made with FW3 as the matrix resin, cured to doses ranging from 0.1 to 1000 kGy. The maximum T_g for the FW3 composite (using sized AS4 fibre), based on the tan δ curve, is about 185°C, occurring at a dose of about 300 kGy. The gel fraction of the matrix polymer at this dose is ~99%, The dose of 300 kGy, using X-ray treatment, also produces a gel content in the matrix polymer of ~99%. The SEC data shows that the molecular weight distribution of the extractables is continually changing, up to the maximum dose studied (1000 kGy), although the changes between 200 and 1000 kGy are minor.

The crosslink density (ν) and the average molecular weight between crosslinks (M_c) were also estimated for the FW3 polymer, from the equilibrium elastic modulus (G'_e), as described above. A plot of the flexural modulus of the neat polymer, as a function of temperature and dose (Fig. 23), shows that the G'_e varies from 6×10^7 to 1×10^8 Pa over the dose range

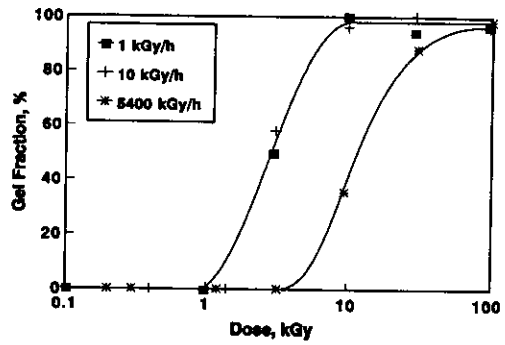

Fig. 16. Dose rate effect on the gel fraction of the S-604 (polypropylene glycol monomethacrylate) resin.

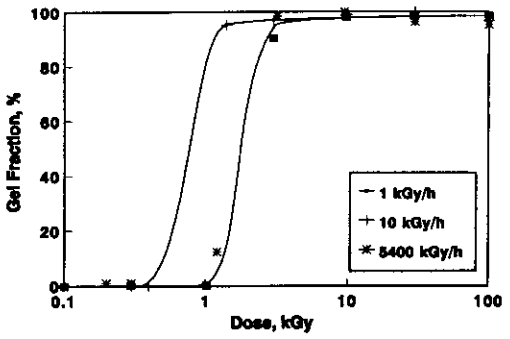

Fig. 17. Dose rate effect on the gel fraction of the CN964 (acrylated urethane) resin.

of 30–1000 kGy. At room temperature, the typical flexural modulus for the FW3 polymer is about 2.52 GPa. The density of the cured resin is 1.237 g/cm^3. Figure 24 shows a plot of the crosslink density of the FW3 polymer as a function of the electron dose. The crosslink density increases with dose, reaching its maximum of about 2.5×10^{-3} mol/cm^3 at a dose of 100–300 kGy. The data in Fig. 24 shows how the molecular weight between the crosslinks of the FW3 polymer varies with dose. The minimum molecular weight between the crosslinks is about 500 Dalton. The molecular weight between the crosslinks for the neat resin and the composite do not show any difference. In the case of FW3, the carbon fibre does not appear to affect the curing of the resin.

Figure 25 shows the data on the flexural modulus of the composite with the FW3 resin, as a function of dose and temperature. The typical flexural modulus for the composite is about 35 GPa, at room temperature, with the elastic modulus varying from about 14–20 GPa, depending on the dose (30–1000 kGy).

Effect of fibre sizing on the curing dose

We have found that the sizing on the fibre has a significant effect on the curing dose for the acrylated

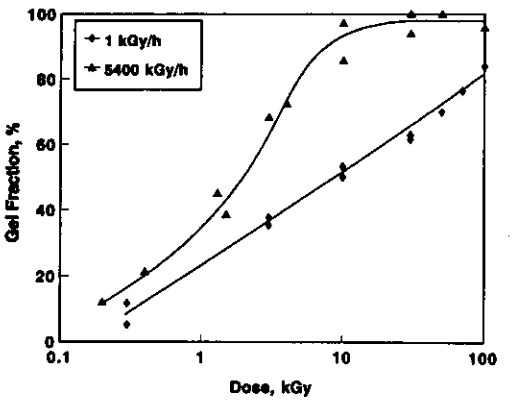

Fig. 18. Dose rate effect on the gel fraction of the C-3000 (epoxy diacrylate oligomer) resin.

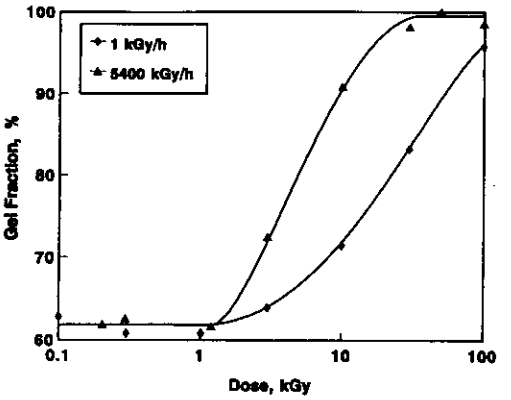

Fig. 19. Dose rate effect on the gel fraction of the C-3000 (epoxy dicrylate oligomer) matrix in a carbon fibre-reinforced composite.

resins. The fibres we have used are from Hercules and come with a *G* sizing on them. This sizing may be an uncured epoxy resin. We have found that with the FW3 acrylated epoxy or BMI4 acrylated bismaleimide, the dose required to cure is approximately 170 kGy. When the same resins are used with unsized fibre, the dose to cure is approximately 70 kGy. The sizing appears to interfere with the free radical curing of the matrix; similar interference was also seen when aramid fibre-reinforced composites were electron-cured (Saunders *et al.*, 1991c); however, in the case of the aramid fibre, the organic fibre itself appears to be a free radical inhibitor.

Effect of a surface coupling agent on composite mechanical properties

Surface treatment of the carbon fibre can play an important role in achieving acceptable bond strengths. The treatment of the fibre surface can take many forms. A coupling agent may be used to enhance chemical bonding between the fibre and the resin. We used a proprietary chemical, an acrylated isocyanate, which was applied at a 1% loading using

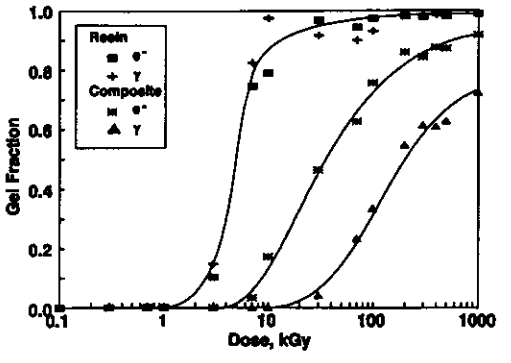

Fig. 20. Gel fraction of BMI1 on irradiation as neat resin, and as matrix in AS4 plain weave unsized fibre-reinforced composite.

Table 2. Crosslink constants for electron cured resins

Resin	T_{go} (°C)	k_1 (°C cm^3 mol^{-1})	k_2 (°C g mol^{-1})
CN104	48.2	37,400	45,900
FW3	10.5	66,300	81,600
BMI1	153.5	12,400	19,600

a solvent method. A heating step was used to chemically bond the isocyanate coupling agent and active sites on the fibres. The acrylated resin was then applied and cured with a dose of 50 kGy.

Scanning Electron Microscopy (SEM) micrographs for the untreated and treated fibre surfaces after fracture have been published (Lopata *et al.*, 1994). The fibres with no coupling agent are clean, showing no adhesion between the fibres and the resin. On the other hand, the fibres treated with the coupling agent have resin adhering to them, illustrating the enhanced bonding between the fibre and the resin matrix.

The use of a coupling agent greatly increases the mechanical properties of the composite. Table 3 shows a comparison of the mechanical properties of the composite samples made from the sized and unsized AS4 fibre with CN104 as the matrix resin. The use of the coupling agent with the sized fibre gives the most significant increase in the mechanical properties. It was expected that the unsized fibre would have given the same increase in mechanical properties, which was not shown by the results. The reason for the difference between the sized and unsized fibres can be attributed to the number of active sites on the fibre with which the coupling agent can react. The sizing on the fibre most likely protects these active sites. The use of acetone as a solvent to apply the agent may dissolve the sizing on the fibre making the active sites available for reaction. In the case of the unsized fibre, these active sites may disappear over time due to exposure to the environment, making the application of the coupling agent ineffective. Although the application of the coupling agent on the sized fibre gives more acceptable mechanical properties, the dose required to cure the composite is higher, by a factor of as much as 3. It is possible that if the coupling agent is applied as a sizing agent during the manufacturing of the fibre, it would also protect the active sites on the fibre (or bond with them); the curing dose for the resulting composite would then be much lower, and the composite formed may show better mechanical properties.

Effect of void content on mechanical properties

We have tried to reduce the void content of the electron-cured composites. The sizing was removed by treating the fibre with hot chromic acid, washing with distilled water and drying in an oven at 150°C for 24 h. An additional step was added in the normal fabrication of the composites with FW3 or CN104 as the resins. The vacuum-bagged composite was heated to 80°C for 4 h to reduce the viscosity of the resin. At 80°C the viscosity for FW3 resin is 0.6 Pa compared with 900 Pa at room temperature. The excess resin was allowed to bleed into a breather cloth. The void content for these composites was lower. This was determined by C-scan (Henneke, 1987) which showed less voids. The void content is ~4% compared to previous panels whose void content was up to 8%. The mechanical properties obtained for these panels are shown in Table 4. As the data shows, the mechanical properties have improved with the reduction of the void content. Further improvement of the mech-

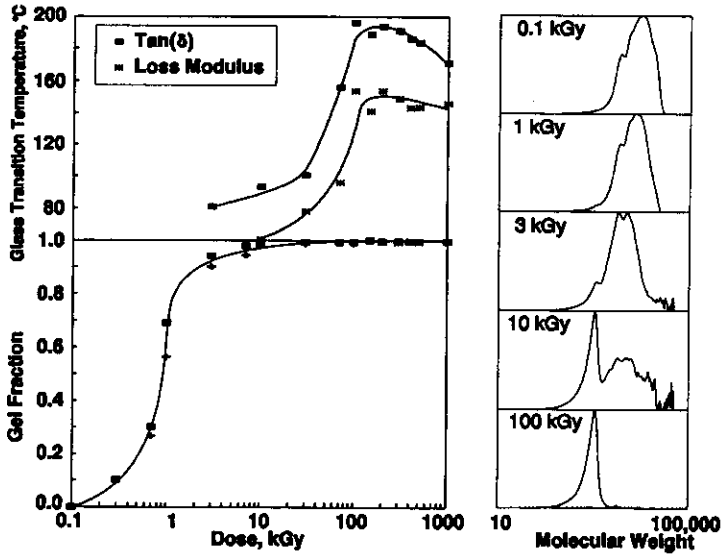

Fig. 21. Effect of dose on the gel fraction, glass transition temperature, and molecular weight distribution of the THF extract of the electron-cured FW3 acrylated epoxy resin.

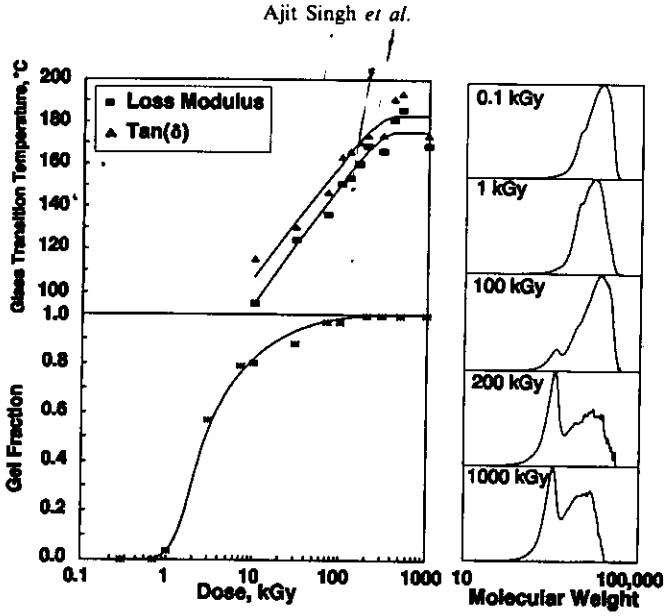

Fig. 22. Effect of dose on the gel fraction, glass transition temperature, and molecular weight distribution of the THF extract of the electron-cured FW3 acrylated epoxy matrix in a carbon fibre-reinforced composite.

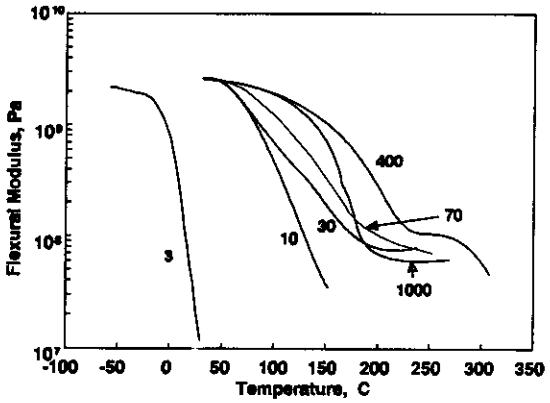

Fig. 23. Effect of dose (in kGy, shown by the numbers beside the curves) on the flexural modulus of the FW3 acrylated epoxy resin. The curves for 100–500 kGy are very close to each other.

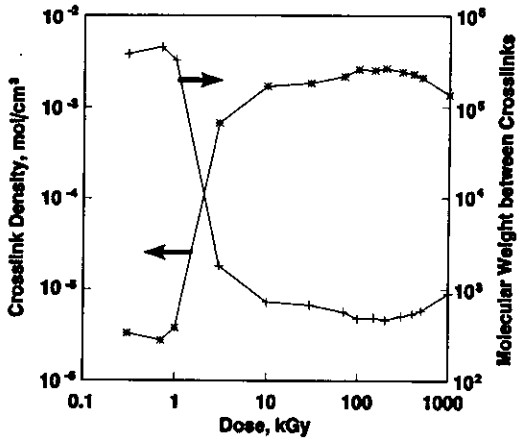

Fig. 24. Effect of dose on the crosslink density and molecular weight between the crosslinks for the FW3 acrylated epoxy resin.

anical properties should occur with the use of the coupling agent, which is planned.

CONCLUDING REMARKS

During our work on electron curing of carbon fibre-reinforced composites, we have identified various advantages offered by this technology and demonstrated some of the key advantages, e.g. reduced stress. The empirical method for curing dose determination, developed by us, enables a rapid screening of the curing dose required for a new resin or formulation. The temperature rise during electron curing can be kept low, if required, either by fractional irradiation or by converting the electron beam into X-rays and curing the samples with X-rays. On the whole, our work on these and other aspects, e.g.

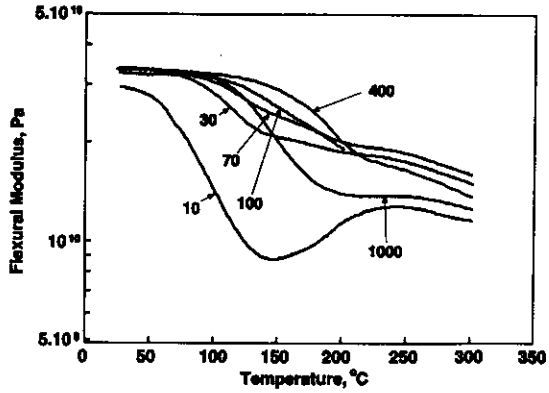

Fig. 25. Effect of dose in kGy (given by the numbers beside the curves) on the flexural modulus of the carbon-fibre-reinforced composite with the FW3 (acrylated epoxy) matrix. The curves for 150–500 kGy are very similar.

Table 3. Effect of acrylated isocyanate coupling agent on the mechanical properties of electron-cured composite with the CN104 resin matrix

Mechanical property	Sized fibre		Unsized fibre	
	No primer	Primer	No primer	Primer
Compression				
Modulus (GPa)	56	60	45	46
Strength (MPa)	156	320	129	151
Flexural				
Modulus (GPa)	48	56	39	43
Strength (MPa)	349	643	256	279
Tensile				
Modulus (GPa)	60	95	95	85
Strength (MPa)	465	805	400	515

Table 4. Effect of void content on mechanical properties for selected electron-cured composites

Resin and loading	Compression		Flexural		Tensile	
	Modulus (GPa)	Strength (MPa)	Modulus (GPa)	Strength (MPa)	Modulus (GPa)	Strength (MPa)
Reduced Void Content (~4%)						
FW3, 35%	64	302	60	375	66	600
FW3, 40%	65	349	64	399	77	695
CN104, 35%	65	251	63	350	74	741
Void Content ~8%						
FW3, 35%	62	140	51	240	55	582
CN104, 35%	46	116	45	301	51	452

dose rate effect, void content and use of a coupling agent, should help provide better understanding of the electron curing technology and thus help its commercialization.

Acknowledgements—The financial support of part of this work by the Defence Research Establishment Pacific, Victoria, BC, is gratefully acknowledged. We thank Professor J. Silverman for helpful comments on the manuscript. We also thank AECL Accelerators, the manufacturers of the 10 MeV electron accelerator (IMPELA), for their interest and generous support of this work.

REFERENCES

ACGIH (1993) *Threshold Limit Values for Chemical Substances and Physical Agents in the Work Environment with Intended Changes for* 1993. American Conference of Governmental and Industrial Hygienists, Cincinnati, Ohio.

ASTM (1984) *Annual Book of ASTM Standards*, Section 8. American Society for Testing and Materials, Pa.

Barnard J. W. and Stanley F. W. (1989) Startup of the Whiteshell Irradiation Facility. *Nucl. Instrum. Methods Phys. Res.* **B40/41**, 1158.

Barnard J. W. and Wilkin G. B. (1987) Safety considerations for a general purpose industrial accelerator facility. *Proc. 20th Midyear Topical Symp. Health Phys. Soc. Health Physics of Radiation Generating Machines*, Reno, Nev.

Beziers, D. and Capdepuy, B. (1990) Electron beam curing of composites. *Proc. 35th Int. SAMPE Conf.*, p. 1221. Anaheim, Calif.

Brynjolfsson A. and Martin T. G. III (1971) Bremsstrahlung production and shielding of static and linear electron accelerators. Toxic gas production, required exhaust rates and radiation protection instrumentation. *Int. J. Appl. Radiat. Isot.* **22**, 29.

Chapiro A. (1962) *Radiation Chemistry of Polymeric Systems*. Interscience, New York.

Charlesby A. (1960) *Atomic Radiation and Polymers*. Pergamon Press, Oxford.

Cook P. M. (1990) Impact and benefit of radiation technology. *Radiat. Phys. Chem.* **35**, 7.

Crivello J. V., Fan M. and Bi D. (1992) Cationic e-beam cure of epoxy resins. *Proc. RADTECH '92*, p. 535.

Dickson L. W. and Singh A. (1987) Radiation curing of epoxies. *Radiat. Phys. Chem.* **31**, 587.

Dole M. (Ed.) (1972, 1973) *The Radiation Chemistry of Macromolecules*, Vols I and II, Academic Press, New York.

Dostal C. A. (Ed.) (1987) *Composites, Engineered Materials Handbook*, Vol. 1. ASM International, Ohio.

Ferry, J. D. (1970) *Viscoelastic Properties of Polymers*, 2nd edition. John Wiley and Sons, New York.

Fila J. A. and Fews R. C. (1993) Civil certification methodology for composite materials in primary aircraft structure. Presented at CANCOM '93, *2nd Canadian Int. Conf. on Composites*, Ottawa.

Henneke II E. G. (1987) Destructive and Nondestructive Tests. In *Composites. Engineered Materials Handbook*, Vol. 1, (Edited by Dostal, C. A.), p. 774. ASM International, Ohio.

IAEA (1982) *Basic Safety Standards for Radiation Protection*. Safety Series No. 9. International Atomic Energy Agency, Vienna.

IAEA (1992) *Radiation Safety of Gamma and Electron Irradiation Facilities*. Safety Series No. 107. International Atomic Energy Agency, Vienna.

ICRP (1960) *Report of Committee II on Permissible Dose for Internal Radiation*, ICRP Publication 2. Pergamon Press, Oxford.

Iverson S. L., Saunders C. B., McDougall T. E., Kremers W., Lopata V. J., Singh. A. and Kerluke D. (1992) Radiation curable composites; environmental advantages. *Proc. Int. Symp. Appl. Isot. Radiat. Conservation Environ.*, Karlsruhe, Germany, p. 223. International Atomic Energy Agency, Vienna.

Kerluke D. R. and McKeown J. (1993) The commercial launch of IMPELA™. *Radiat. Phys. Chem.* **42**, 511.

Kroh J. (Ed.) (1989) *Early Developments in Radiation Chemistry*. Royal Society of Chemistry, Cambridge.

Lapin S. C. (1986) Electron beam activated cationic curing of vinyl ethers. *Proc. RADCURE '86*, pp. 15–15.

Laramee R. C. (1987) Selection and evaluation of composite. In *Composites, Engineered Materials Handbook*

(Edited by Dostal C. A.), Vol. 1, p. 38. ASM International, Ohio.

Leemhorst J. G. and Miller A. (Eds) (1990) Proceedings 7th International Meeting on Radiation Processing. *Radiat. Phys. Chem.* **35**.

Lopata V. J., Chung M., McDougall T. E. and Weinberg V. A. (1994) Electron-curable adhesives for high-performance structures. *Proc. 39th SAMPE Conf.*, p. 514. Anaheim, Calif.

Luck R. M. and Sadhir R. K. (Eds) (1992) Shrinkage in conventional monomer during polymerization. *Expanding Monomer, Synthesis, Characterization, and Applications* (Edited by Luck R. M. and Sadhir R. K.) p. 1. CRC Press, Boca Raton, Fla.

Margolis J. M. (Ed.) (1986) *Advanced Thermoset Composites*. Van Nostrand Reinhold, New York.

Mayer J., Cassel R. and Twombly B. (1990) Advanced Mechanical Analysis Techniques for Viscoelastic Characterization of Polymers. *Am. Lab.* **22**, 60.

NBS (1973) *Photonuclear Reaction Data*. NBS Special Publication 380. National Bureau of Standards (National Institute of Standards and Technology), Washington, D.C.

NCRP (1977) *Radiation Protection Design Guidelines for 0.1–100 MeV Particle Accelerator Facilities*. NCRP Report No. 51. National Council on Radiation Protection and Measurements, Washington, D.C.

Nucleon Lectern (1984) *The Health Physics and Radiological Health Handbook*. Nucleon Lectern, Olney, Md.

Pater R. H., Whitley K., Morgan C. and Chang C. (1991) Crosslinking-property relationships in PMR polyimide composites. *Polym. Comp.* **12**, 126.

Rheometrics Inc. (1990) *Understanding Rheological Testing*. Piscataway, N.J.

Sadhir R. K. and Luck R. M. (Eds) (1992) *Expanding Monomers, Synthesis, Characterization, and Applications*, CRC Press, Boca Raton, Fla.

Saunders C. B. (1988) *Radiation Processing in the Plastics Industry: Current Commercial Applications*. Atomic Energy of Canada Limited Report, AECL-9569.

Saunders C. B. and Singh A. (1989) *The Advantages of Electron-Beam Curing of Fibre-Reinforced Composites*. Atomic Energy of Canada Limited Report, RC-264. Available from Scientific Document Distribution Office (SDDO), Atomic Energy of Canada Limited, Chalk River, Ontario K0J 1IJ0.

Saunders C. B., Singh A. and Czvikovszky T. (1991a) Radiation processing of fibre-reinforced composites. *Proc. 12th Ann. Can. Nucl. Soc. Meeting*, p. 64.

Saunders C. B., Lopata V. J., Kremers W., Tateishi M. and Singh A. (1992) Recent developments in the electron-beam curing of fiber-reinforced composites. *Proc. 37th Int. SAMPE Conf.* p. 944. Anaheim, Calif.

Saunders C. B., Dickson L. W., Singh A., Carmichael A. A. and Lopata V. J. (1988a) *Radiation-Curable Prepreg Composites*. Atomic Energy of Canada Limited Report, AECL-9560.

Saunders C. B., Dickson L. W., Singh A., Carmichael A. A. and Lopata V. J. (1988b) Radiation-Curable Carbon Fiber Prepreg Composites. *Polym. Comp.* **9**, 389.

Saunders C. B., Carmichael A. A., Kremers W., Lopata V. J. and Singh A. (1991b) Radiation-curable prepreg composites. *Polym. Comp.* **12**, 91.

Saunders C .B., Singh A., Lopata V. J., Kremers W. and Tateishi M. (1993a) Characterization of matrix polymers for electron-beam-cured fiber-reinforced composites. In *Irradiation of Polymeric Materials*, (Edited by Reichmanis E., Frank C. W. and O'Donnell J. H.), p. 305. American Chemical Society, Washington, D.C.

Saunders C. B., Lopata V. J., Kremers W., McDougall T. E., Tateishi, M. and Singh A. (1993b) Electron curing of fiber-reinforced composites; recent developments. *Proc. 38th SAMPE Conf.*, p. 1681. Anaheim, Calif.

Saunders C. B., Lopata V. J., Kremers W., McDougall T. E., Chung M. and Barnard J. W. (1994) Electron and X-ray curing of thick composite structures. *Proc. 39th SAMPE Conf.*, p. 486. Anaheim, Calif.

Saunders C. B., Singh A., Lopata V. J., Seier S., Boyer G. D., Kremers W. and Mason V. A. (1991c) Electron beam curing of aramid-fiber reinforced composites. In *Radiation Effects on Polymers* (Edited by Clough, R. L. and Shalaby S. W.), p. 251. ACS Symp. Ser. 475, American Chemical Society, Washington. D.C.

Schroeder K. F. (1990) Radiation curing in Europe; 1989 market overview and trends. *Beta-Gamma*, **1**, 10.

Silverman J. (1981) Radiation processing—the industrial applications of radiation chemistry. *J. Chem. Educ.* **58**, 168.

Singh A. and Saunders C. B. (1992) Radiation processing of carbon-fiber acrylated epoxy composites. In *Radiation Processing of Polymers* (Edited by Singh A. and Silverman J.), p. 187. Hanser, Munich.

Singh A. and Silverman J. (1992) Radiation processing: an overview. In *Radiation Processing of Polymers* (Edited by Singh A. and Silverman J.), p. 1. Hanser, Munich.

Singh A., Lopata V. J., Kremers W., McDougall T. E., Tateishi M. and Saunders C. B. (1993) Electron-cured fibre-reinforced advanced composites. *Proc. CANCOM'93* (Edited by Wallace W., Gauvin R. and Hoa S. V.), p. 277. Ottawa.

Stannett V. T., Silverman J. and Garnett J. L. (1989) Polymerization by high-energy radiation. In *Comprehensive Polymer Science* (Edited by Eastmond G. C., Ledwith A., Russo S. and Sigwalt P.), Vol. 4, p. 317. Pergamon Press, Oxford.

Swanson W. P. (1979) *Radiological Safety Aspects of the Operation of Electron Linear Accelerators*. Technical Report Series No. 188. International Atomic Energy Agency, Vienna.

Tabata Y. (1990) Radiation curing in Japan. *Beta-Gamma* **1**, 6.

Tenorth Y. (1990) Designing and realization of a modern EBC-plant for coating wood-cement and particle boards. *Beta-Gamma* **1**, 32.

Traceski F. T. (1987) Guide to general information sources. In *Composites, Engineered Materials Handbook* (Edited by Dostal C. A.), Vol. 1, p. 38. ASM International, Ohio.

Walton T. C. and Crivello J. V. (1994) Innovative composite fabrication using electron-beam rapidly cured, micrometeoride and atomic oxygen resistant EFS polymers. *Proc. 39th SAMPE Conf.* (Edited by Drake K., Bauer J., Serafini T. and Cheng P.), p. 497. Anaheim, Calif.

Weeton J. W., Peters D. M. and Thomas K. L. (1987) *Engineers' Guide to Composite Material*. American Society of Metals, Ohio.

Williams T. F. (1968) Radiation induced polymerization. *Fundamental Processes in Radiation Chemistry* (Edited by Ausloos P.), p. 515. Interscience, New York.

Wilson J. E. (1974) *Radiation Chemistry of Monomers, Polymers, and Plastics*. Marcel Dekker, New York.

Woods R. J. and Pikaev A. K. (1994) *Applied Radiation Chemistry: Radiation Processing*. Wiley, New York.